# Supplemental Material for " Backscattering-immune optomechanical entanglement in a whispering-gallery-mode resonator"

Bo Zhao,[1,2] Mei-Rong Wei,[1,2] and Qi Guo[1,2,*]

[1]*State Key Laboratory of Quantum Optics and Quantum Optics Devices,*
*Institute of Opto-Electronics, College of Physics and Electronic Engineering,*
*Shanxi University, Taiyuan, Shanxi 030006, China*
[2]*Collaborative Innovation Center of Extreme Optics, Shanxi University, Taiyuan 030006, China*

The Supplemental Material is organized as follows. In Section SI, we present detailed calculation of eigen frequencies. In Section SII, we analyze stability of the system based on numerical calculation. In Section SIII, we present enhancement of the robustness against environmental temperature and optical dissipation compared to the case without nanoparticle. In Section SIV, we study backscattering-immune intracavity photon number and EPR steering. In Section SV, we show the revival from backscattering for non-Hermitian case.

## SI.  DETAILED CALCULATION OF EIGEN FREQUENCIES

First, we consider the Hamiltonian of the optical modes, including dissipation, which can be written in matrix form:

$$\begin{pmatrix} \hbar(\omega_c + \epsilon + \eta) - i\hbar\Gamma & \hbar J_1 \\ \hbar J_2 & \hbar(\omega_c + \epsilon + \eta) - i\hbar\Gamma \end{pmatrix}. \tag{S1}$$

By solving the secular equation $\det(H - \hbar\omega I) = 0$, we can obtain the eigen frequencies:

$$\begin{aligned} \omega_{1,2} &= \omega_c - i\Gamma + \epsilon + \eta \pm \sqrt{J_1 J_2} \\ &= \omega_c - i\Gamma + \epsilon + \eta \pm \sqrt{\epsilon^2 + \eta^2 + 2\epsilon\eta\cos(2m\beta)}, \end{aligned} \tag{S2}$$

where $\omega_{1,2}$ represents the eigen frequencies of the optical modes, and $I$ is the identity matrix.
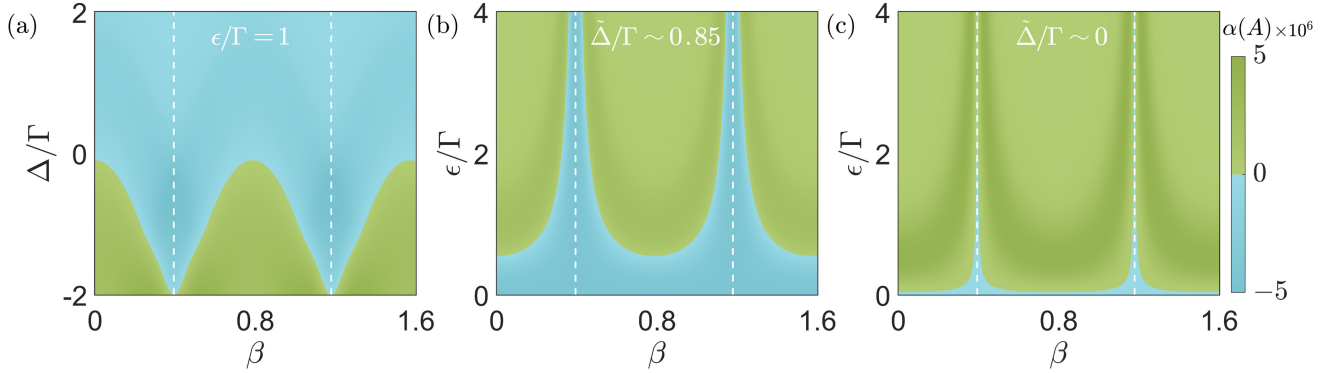


FIG. S1. Stability analysis of the system. (a) Spectral abscissa, $\alpha(A)$, versus relative angle, $\beta$, and $\Delta/\Gamma$. The parameters are the same as those in Figs. 3(a), 3(c) and 3(e). (b) Spectral abscissa, $\alpha(A)$, versus relative angle, $\beta$, and $\Delta/\Gamma$. The parameters are the same as those in Figs. 3(b) and 3(d). (c) Spectral abscissa, $\alpha(A)$, versus relative angle, $\beta$, and $\Delta/\Gamma$. The blue regions indicate a negative spectral abscissa (system is stable), while the green regions indicate a non-negative spectral abscissa (system is unstable). The parameters are the same as those in Fig. 3(f). The white dashed lines denote $\beta = \beta_{\mathrm{Im}}$.

## SII. STABILITY ANALYSIS

According to Routh-Hurwitz criterion [85], the system is stable and reaches its steady state when all eigenvalues of the coefficient matrix, $A$, have negative real parts. Because eigenvalues of the coefficient matrix, $A$, can be easily obtained through numerical calculation, we numerically analyze the system's stability as shown in Fig. S1. Fig. S1(a) shows the systems stability for the parameters in Figs. 3(a), 3(c), and 3(e); Fig. S1(b) corresponds to the parameters in Figs. 3(b) and 3(d); and Fig. S1(c) corresponds to the parameters in Fig. 3(f). The blue regions mean that spectral abscissa of the coefficient matrix, $\alpha(A) = \max\{\text{Re}(\lambda) \mid \lambda \in \text{Eigenvalues of } A\}$, is less than 0, which shows that the system is stable and tends toward a steady state. Though there exist some unstable regions in Fig. S1, they do not affect the discussions and conclusions of the main text. Especially, when $\beta \sim \beta_{\text{Im}}$, the system revives to stable for a given effective optical detuning as shown in Figs. S1(b) and S1(c).

## SIII. ROBUSTNESS ENHANCEMENT

Thermal noise and optical dissipation are significant factors which can destroy quantum correlations. In this section, we study the robustness of the optomechanical entanglement between the driven optical mode and the mechanical mode against environmental temperature and optical dissipation. By comparing the cases with and without a nanoparticle, we find that by introducing the nanoparticle with proper position, not only can the entanglement revive (as shown in the main text), but also the robustness of the entanglement is greatly enhanced.

Figure S2 shows the effect of environmental temperature on optomechanical entanglement. We plot the maximum optomechanical entanglement, $E_{\mathcal{N},r}^{max}$, versus environmental temperature, $T_e$, in Fig. S2(a). The green dashed line denotes the system with defect ($\epsilon = \Gamma$), and the blue solid line denotes the system with both defect and nanoparticle ($\epsilon = \eta = \Gamma$, $\beta = \beta_{\text{Im}}$). We find the optomechanical entanglement, $E_{\mathcal{N}}$, can exist at higher temperature in the system with nanoparticle than the system without nanoparticle. The honeydew shadow means the robustness enhancement area against environmental temperature and the optomechanical entanglement exists even at $T_e \sim 3.6$ K in the system with nanoparticle. We also plot the optomechanical
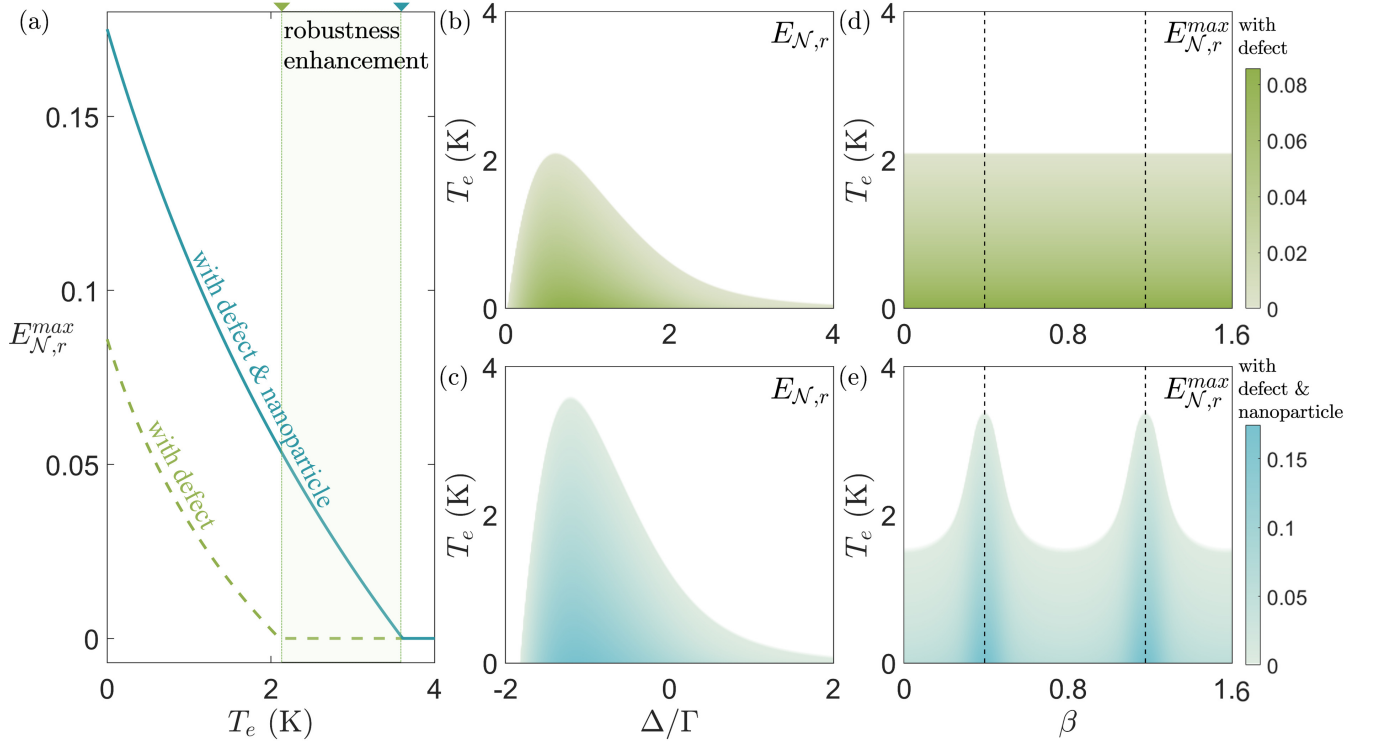


FIG. S2. (a) Maximum optomechanical entanglement, $E_{\mathcal{N},r}^{max}$, versus environmental temperature, $T_e$. Optomechanical entanglement, $E_{\mathcal{N},r}$, for the defective system without nanoparticle (b) and with nanoparticle (c) versus $\Delta/\Gamma$ and environmental temperature, $T_e$. $\beta = \pi/8$ in (c). Maximum optomechanical entanglement, $E_{\mathcal{N},r}^{max}$, for the defective system without nanoparticle (d) and with nanoparticle (e) versus relative angle, $\beta$, and environmental temperature, $T_e$. Other parameters are the same as those in Fig. S1(a).
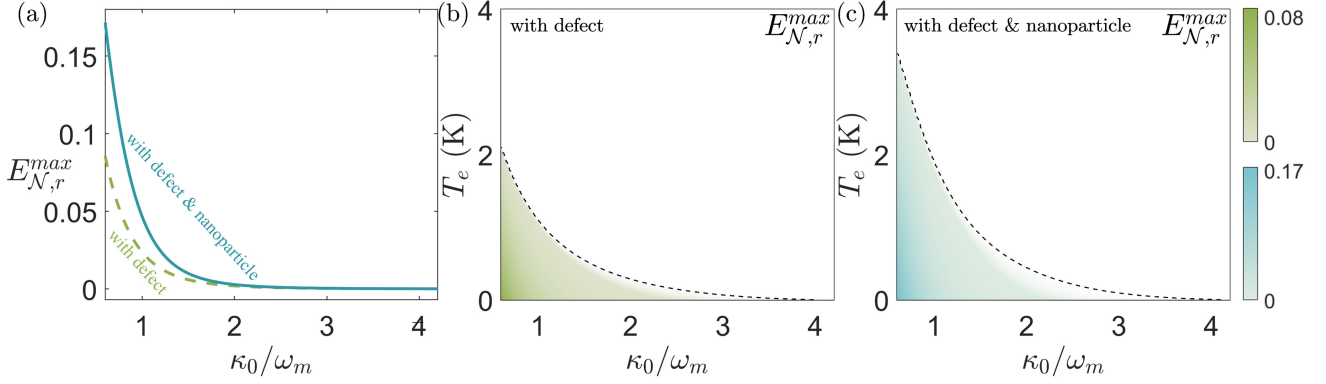
FIG. S3. (a) Maximum optomechanical entanglement, $E_{\mathcal{N}}^{max}$, versus optical dissipation, $\kappa_0/\omega_m$. Maximum optomechanical entanglement, $E_{\mathcal{N}}^{max}$, versus optical dissipation, $\kappa_0/\omega_m$, and environmental temperature, $T_e$, for the defective system without nanoparticle(b) and with nanoparticle(c). $\epsilon = 0.6\omega_m$, other parameters are the same as those in Fig. S1(a).

entanglement, $E_{\mathcal{N},r}$, for the defective system without nanoparticle and with nanoparticle versus $\Delta/\Gamma$ and environmental temperature, $T_e$, in Figs. S2(b) and S2(c), respectively, and the corresponding maximum optomechanical entanglement, $E_{\mathcal{N},r}^{max}$, versus relative angle, $\beta$, and environmental temperature, $T_e$, in Figs. S2(d) and S2(e), to show the robustness enhancement against environmental temperature. Clearly, the optimal robustness enhancement against environmental temperature emerges at an angle of $\beta = \beta_{\mathrm{Im}}$.

Then we study the robustness enhancement against optical dissipation. We plot the maximum optomechanical entanglement, $E_{\mathcal{N},r}^{max}$, versus optical dissipation, $\kappa_0/\omega_m$, in Fig. S3(a) for cases with and without nanoparticle ($\beta = \beta_{\mathrm{Im}}$), which shows the robustness against optical dissipation can be enhanced by introducing the nanoparticle with proper position. We also plot the maximum optomechanical entanglement, $E_{\mathcal{N}}^{max}$, versus optical dissipation, $\kappa_0/\omega_m$, and environmental temperature, $T_e$, in Figs. S3(b) and S3(c) for the defective system without and with nanoparticle, respectively. Comparing Figs. S3(b) and S3(c), it is clear that the robustness of optomechanical entanglement, $E_{\mathcal{N},r}$, in the system with an appropriate nanoparticle against both thermal noises and optical dissipation is enhanced.

## SIV.  BACKSCATTERING-IMMUNE EFFECTS

In this section, we show the backscattering-immune intracavity photon number of CW mode and the backscattering-immune EPR steering at $\beta = \beta_{\mathrm{Im}}$.
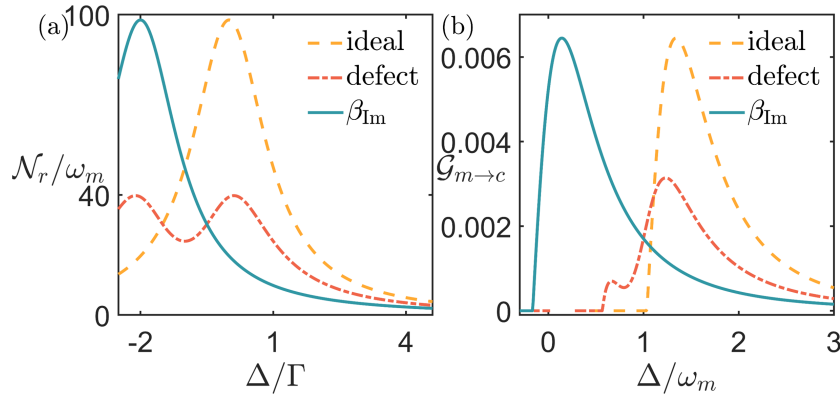


FIG. S4. (a) Intracavity photon number of the driven mode, $\mathcal{N}_r$, versus $\Delta/\Gamma$. (b) EPR steering, $\mathcal{G}_{m \to c}$, versus $\Delta/\Gamma$. Backscattering immunity emerges for the case of $\beta = \beta_{\mathrm{Im}}$. See text for the parameters.

The intracavity photon number of CW mode can be obtained from Eq. (9):

$$\mathcal{N}_r = |\alpha|^2 = \left| \frac{(i\tilde{\Delta} + \Gamma)\varepsilon}{(i\tilde{\Delta}+\Gamma)^2 + J_1 J_2} \right|^2. \tag{S3}$$

And the EPR steering can be obtained from the correlation matrix in Eq. (12). Here, we consider the EPR steering from the mechanical mode to the CW mode, which can be quantified as [94]

$$\mathcal{G}_{m \to c} = \max[0, S(2\mathcal{A}) - S(2V')], \tag{S4}$$

where $S(\sigma) = [\ln \det(\sigma)]/2$ ($\sigma = 2\mathcal{A}, 2V'$). $\mathcal{G}_{m \to c} > 0$ means the presence of EPR steering from the mechanical mode to the CW mode, and the value of $\mathcal{G}_{m \to c}$ represents the strength of the steerability. In Figs. S4(a) and S4(b), we show the backscattering-immune intracavity photon number of CW mode and backscattering-immune EPR steering from mechanical mode to CW mode, respectively. In Fig. S4(a), the parameters we choose are the same as those in Fig. 2(a). In Fig. S4(b), the parameters we choose are: $\mu = 10$ ng, $R = 1.1 \times 10^{-3}$ m, $T = 0$ K, $\omega_m = 63 \times 10^6$ Hz, $\gamma_m = 0.1\omega_m$, $\omega_c = 1.22 \times 10^{15}$ Hz, $\kappa_0 = 0.1\omega_m$, $\kappa_{ex} = \kappa_0$ and $P = 50$ mW.

## SV.  NON-HERMITIAN CASE

If we consider complex $\epsilon$ and $\eta$, $\epsilon/\Gamma = \eta/\Gamma = 1 - 0.05i$, the system becomes non-Hermitian, and the total optical dissipation will be $\Gamma - \mathrm{Im}(\epsilon + \eta)$. As shown in Fig. S5, the revival from backscattering can also be achieved for the non-Hermitian system, but we should note that the system cannot revive to the level of the ideal case without defect, which is caused by the extra optical dissipation $\mathrm{Im}(\epsilon + \eta)$ induced by a defect and nanoparticle.
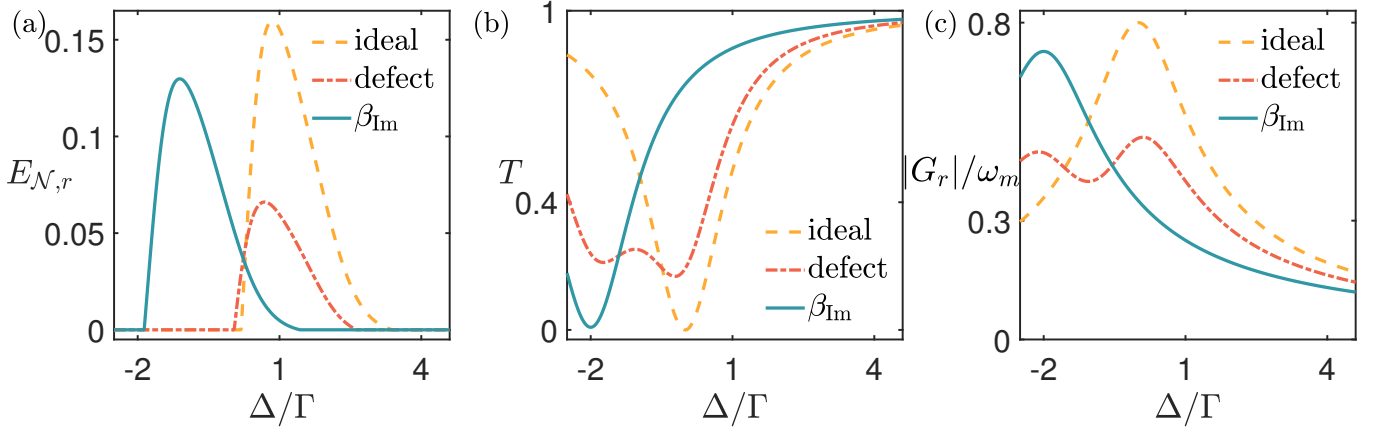


FIG. S5. (a) Optomechanical entanglement, $E_{\mathcal{N},r}$, (b) normalized transmission rate, $T$, (c) effective COM coupling rate, $|G_r|$, versus $\Delta/\Gamma$ for various cases. The optimal revival from backscattering emerges at an angle of $\beta = \beta_{\mathrm{Im}}$. Other parameters are the same as in Fig. S1(a).

[85] E. X. DeJesus and C. Kaufman, Routh-Hurwitz criterion in the examination of eigenvalues of a system of nonlinear ordinary differential equations, Phys. Rev. A **35**, 5288 (1987).

[94] I. Kogias, A. R. Lee, S. Ragy, and G. Adesso, Quantification of Gaussian quantum steering, Phys. Rev. Lett. **114**, 060403 (2015).